Study of the Further Reduction of Shaft Voltage of Brushless DC Motor With Insulated Rotor Driven by PWM Inverter

Yoshinori Isomura, Kichiro Yamamoto, *Member, IEEE*, Shigeo Morimoto, *Member, IEEE*, Tatsuo Maetani, Akihiko Watanabe, and Keisaku Nakano

***Abstract*—The authors previously succeeded in reducing the shaft voltage of a PWM driven motor with a rotor which had an outer core and an inner core (and the shaft), electrically insulated each other by a resin (hereafter, the insulated rotor). This paper proposes a new method for further reduction of the shaft voltage of a motor with an insulated rotor by adding a capacitor between brackets and N line of the dc link of the inverter. A common-mode equivalent circuit of the system with an ungrounded motor is examined, and the effect of further reduction by the new method is verified by calculation of the shaft voltage from the equivalent circuit and measurement of the shaft voltage of the motor.**

***Index Terms*—Bearing current, common-mode voltage, shaft voltage, stray capacitance.**

I. Introduction

As THE need for energy-saving measures increases, the numbers of brushless direct current (BLDC) motors used to drive air-conditioning fans have been rapidly increasing. Also, voltage-source pulsewidth modulation (PWM) inverters, generally used to drive fan motors, have been posing a major problem, which is the high probability of the electrical erosion of bearing in the motors. A potential difference, called shaft voltage, is generated between the outer and inner races by inverter switching, and this voltage causes the dielectric breakdown of the bearing lubricant. The current produced by the dielectric breakdown, also called "electric discharge machining current," results in a current passing through the bearing and causes electrical erosion in the bearing [1]–[13].

Shaft voltage can be suppressed by suppressing either the common-mode voltage causing shaft voltage or the shaft voltage itself. Previously, we proposed an outer core and an inner core (and the shaft), electrically insulated each other by a resin which can suppress the shaft voltage in BLDC motors for air conditioning (hereinafter, this concept is referred to as "insulated rotor") [6], [13]. The insulated rotor can suppress the capacitance of the entire rotor and, hence, the shaft voltage. However, fine tuning of the capacitance of insulated rotor C_d using a resin cast is very difficult.

In this paper, the method of further suppressing shaft voltage by addition of a capacitor to the insulated rotor BLDC motor driven by a PWM inverter is explained. First, shaft voltage is simulated from the equivalent circuit, and it is confirmed that the simulated shaft voltage is in accordance with the measurement result [6]. Next, the structure, which added the capacitor between the brackets and the stator core, is presented. Also, the optimal placement of the capacitor is investigated by simulating shaft voltage.

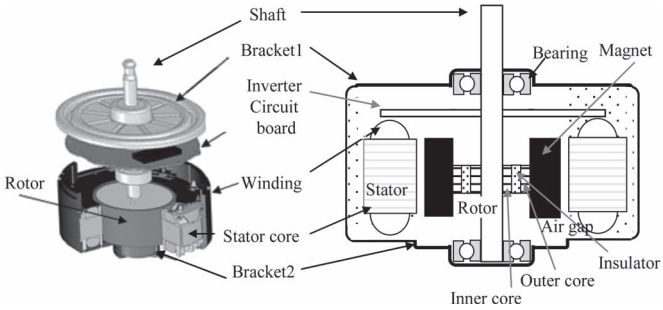

Fig. 1. BLDC motor.

II. Shaft Voltage Reduction of Ungrounded Motor

In this section, the shaft voltage reduction method for ungrounded motors with insulated rotor is explained. This section is almost a summary of [6].

Fig. 1 shows the external view of a concentrated winding BLDC motor used to drive an air-conditioning fan. This motor is a surface permanent magnet synchronous motor where the stator core and stator windings are molded with a resin and a ferrite plastic magnet is also molded on the rotor core surface. Metal brackets are mounted on the top and bottom of the stator to hold the bearing. Both metal brackets are connected to each other inside the motor. The inverter circuit to drive the motor is mounted in the stator of the motor. This motor is ungrounded.

Manuscript received October 9, 2013; revised January 21, 2014; accepted February 19, 2014. Date of publication March 13, 2014; date of current version November 18, 2014. Paper 2013-IDC-695.R1, presented at the 2013 IEEE International Conference on Power Electronics and Drive System, Kitakyushu, Japan, April 22–25, and approved for publication in the IEEE TRANSACTIONS ON INDUSTRY APPLICATIONS by the Industrial Drives Committee of the IEEE Industry Applications Society.

Y. Isomura, T. Maetani, A. Watanabe, and K. Nakano are with the Motor Business Division, Appliances Company, Panasonic Corporation, Daito 574-0044, Japan (e-mail: isomura.yoshinori@jp.panasonic.com; Maetani.tatsuo@jp.panasonic.com; watanabe.aw@jp.panasonic.com; nakano.keisaku@jp.panasonic.com).

K. Yamamoto is with Kagoshima University, Kagoshima 890-0065, Japan (e-mail: yamamoto@eee.kagoshima-u.ac.jp).

S. Morimoto is with Osaka Prefecture University, Sakai 599-8581, Japan (e-mail: morimoto@eis.osakafu-u.ac.jp).

Color versions of one or more of the figures in this paper are available online at http://ieeexplore.ieee.org.

Digital Object Identifier 10.1109/TIA.2014.2311591

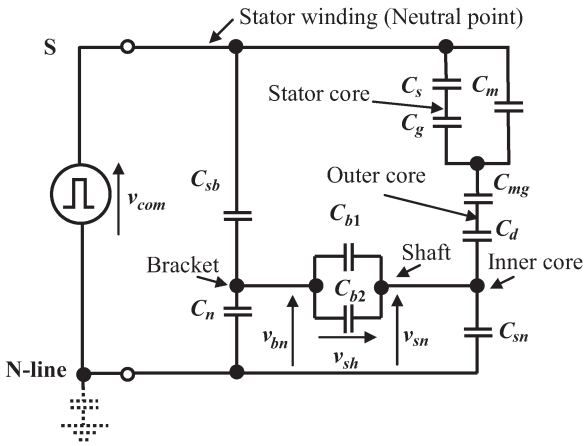

Fig. 2. Bridge-type equivalent circuit of the motor for common mode.

TABLE I
MEASURED CAPACITANCE IN EACH PART OF THE MOTOR

Symbol	Measured part	Measured value
C_s	Stray capacitance; winding to stator core	400pF
C_g	Stray capacitance; stator core to magnet	70pF
C_{mg}	Magnet capacitance	69pF
C_m	Stray capacitance; winding to magnet	8pF
C_b	Bearing capacitance (C_{b1}+C_{b2})	100pF
C_d	Insulated rotor capacitance	4.5pF
C_{sb}	Stray capacitance; winding to bracket	19pF
C_{sn}	Stray capacitance; shaft to N-line	7.7pF
C_n	Stray capacitance; bracket to N-line	20pF

The rated output power of the motor is 60 W, and the inverter operates under two-phase modulation. Two 608-type bearings are used, and each is lubricated by a urea-based lubricant with a base-oil viscosity of 53 mm^2/s.

Fig. 2 shows an ungrounded three-phase common-mode equivalent circuit. The equivalent circuit has a bridge-type structure, and it was developed with consideration of the following facts.

1) The shaft voltage varies depending on the capacitance value of the insulated rotor.
2) The polarities of both common-mode and shaft voltages become reverse when the capacitance of the insulated rotor is very small.

Shaft voltage $v_{\rm sh}$ is generated between the outer and inner races by inverter switching because common-mode voltage $v_{\rm com}$, which is the voltage between a neutral point S of the inverter output voltage and negative potential N of the dc link, is divided by capacitances inside the motor. Because the value of the insulated rotor capacitance C_d is almost infinity in conventional motors without insulator, the potential on the shaft side is higher than that on the bracket side.

The measurement results are listed in Table I [6]. LCR meter ZM2353 manufactured by the NF Corporation was used for the measurements, and as the measurement frequency, 20 kHz (carrier frequency of the inverter) was selected.

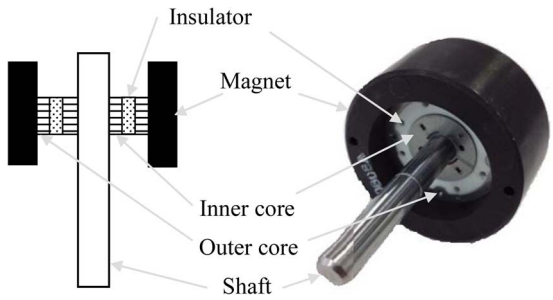

Fig. 3. Insulated rotor structure.

1) Combined capacitance between the winding and the stator core C_s: the capacitance between the neutral point of the stator windings and the stator core was measured.
2) Capacitance between the stator core and the magnet C_g: the capacitance between the stator core and the magnet surface with rotor inserted in unwound stator was measured.
3) Magnet capacitance C_{mg}: the capacitance between the rotor surface and the shaft was measured.
4) Combined capacitance between the winding and the magnet C_m: the rotor was inserted into the stator, and the capacitance between the neutral point and the shaft was measured as the combination of C_m, C_g, and C_{mg}. Then, C_m was calculated.
5) Bearing capacitances C_{b1} and C_{b2}: the capacitances of bearings 608ZZ at 1000 min^{-1}. In this paper, we performed comparison and verification at 1000 min^{-1} which may be used for an air conditioner. The differences for rotational speeds have already been indicated in our previous paper [13].
6) Combined capacitance between the winding and the brackets C_{sb}: the capacitance between the neutral point of the stator winding and the brackets was measured.
7) Combined capacitance between the shaft and the N electric potential C_{sn}: the capacitance between the shaft and the N electric potential of the inverter was measured.
8) Combined capacitance between the N electric potential and the bracket C_n: the bracket and the inverter circuit were inserted into the molded stator only, and the capacitance between the bracket and the inverter was measured.

Fig. 3 shows the structure of the insulated rotor. Outer and inner rotor cores are inserted in the inside of a plastic magnet, and resin is placed between the outer and inner cores. Because the insulated rotor capacitance C_d is small, the potential at the shaft side (v_{sn}) is lower than that of conventional motor without insulator. Choosing the value of C_d so that v_{sn} can be equal to the potential of the bracket v_{bn}, the shaft voltage can be suppressed.

Fig. 4 shows the measurement results of $v_{\rm com}$ and $v_{\rm sh}$ of the motor with an insulated rotor. The dc link voltage was 280 V, the motor rotating speed was 1000 min^{-1}, and the motor was operated with no load. As can be seen from the figure, the bearing lubricant is not dielectrically broken down at the value of the amplitude of $v_{\rm sh}$ (-2.5 V). In addition, the polarity of the shaft voltage is opposite to that of the common-mode voltage.

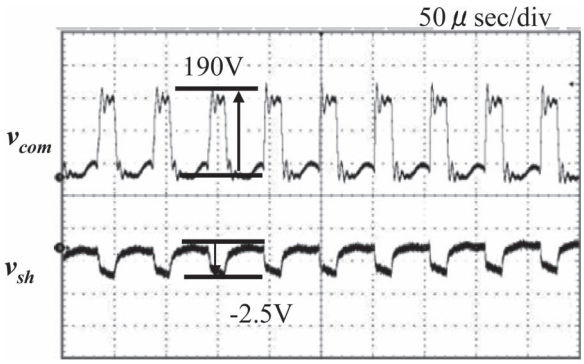

Fig. 4. Measured common-mode voltage $v_{\rm com}$ and shaft voltages $v_{\rm sh}$.

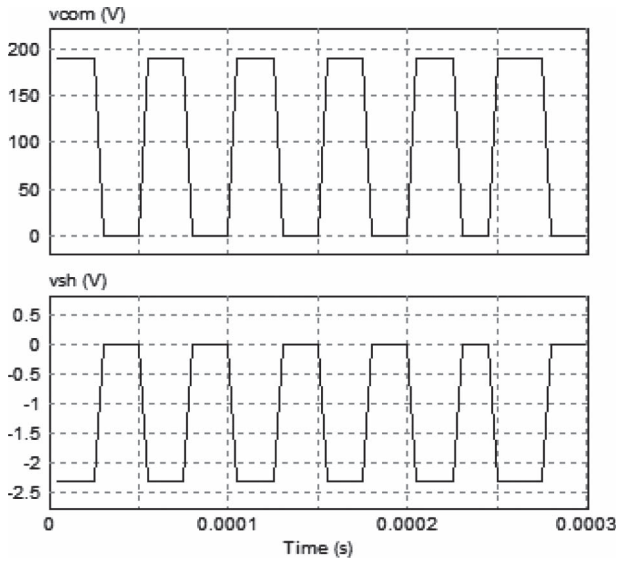

Fig. 5. Simulation results of shaft voltage $v_{\rm sh}$ of the motor with an insulated rotor.

Fig. 5 shows the simulation results of $v_{\rm com}$ and $v_{\rm sh}$ of the motor with an insulated rotor. The conditions of the simulation were made equal to the conditions of the measurement. The results of the measurement and the simulation are mostly in agreement. Therefore, one can find that $v_{\rm sh}$ is equal to zero when the insulated rotor capacitance C_d is precisely produced. However, fine tuning of the capacitance of insulated rotor C_d using a resin cast is very difficult. Therefore, the fine tuning method is examined in the next section.

III. New Further Reduction Method of the Shaft Voltage

A. Common-Mode Equivalent Circuit of the New Method

Fig. 6 shows the capacitive coupling in the BLDC motor. The shaft voltage of the motor $v_{\rm sh}$ is the voltage between the shaft and the bracket and is also the voltage across bearing capacitances C_{b1} and C_{b2}. In addition, the electric potential of the shaft is decided by voltage division of shaft side capacitances C_s, C_g, C_{mg}, C_d, C_m, and C_{sn}, and the potential of the bracket is decided by voltage division of bracket sides C_{sb} and C_n. Based on the bridge equivalent circuit in Fig. 2, the motor was disassembled into each component, such as stator and rotor, and then, capacitances were measured for each respective part exclusively or in combination.

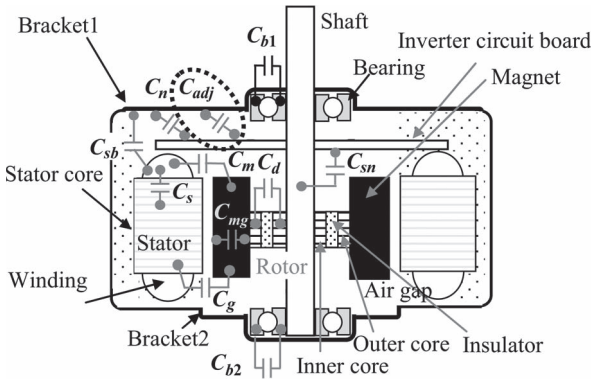

Fig. 6. Motor capacitive coupling.

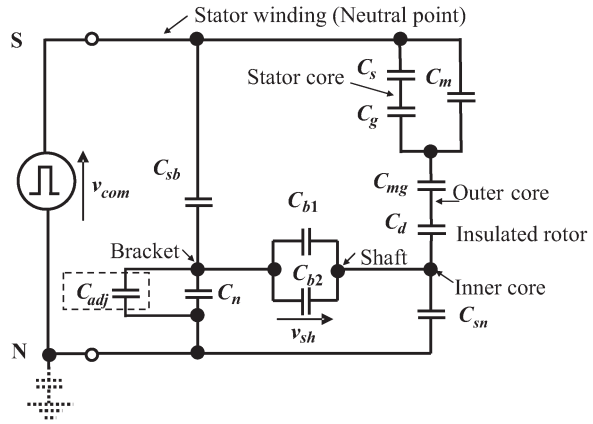

Fig. 7. Bridge-type equivalent circuit of the motor with adjusting capacitor.

In order to reduce the shaft voltage more, we propose adding the adjusting capacitor $C_{\rm adj}$, which is a commercial part of low cost. $C_{\rm adj}$ is placed between the bracket and the N line of the inverter circuit board to reduce the shaft voltage close to 0 V from -2.5 V (Fig. 5). Practically, $C_{\rm adj}$ is arranged to be in parallel with C_n. Fig. 7 is the new bridge-type equivalent circuit in which $C_{\rm adj}$ is added for adjustment of the capacitance.

The feature of this equivalent circuit is the addition of the adjusting capacitor to adjust the electric capacitance decided by the structure of a BLDC motor. The specifications of an air-conditioning motor are listed in Table II.

B. Shaft Voltage Simulation by the Equivalent Circuit

Next, the effects of this new method are checked in a simulation. Fig. 8 shows the simulation results based on the new equivalent circuit. In this case, the dc link voltage was DC280 V, the peak value of $v_{\rm com}$ was DC190 V, and two-phase PWM was used to drive the motor. Moreover, the waveform of $v_{\rm com}$ was given on the basis of an experimental result at 1000 min^{-1}. Fig. 8(a) is the waveform for $C_{\rm adj} = 9$ pF and $v_{\rm sh} = -0.9$ V. Similarly, $v_{\rm sh} = -0.2$ V for $C_{\rm adj} = 15$ pF in Fig. 8(b), $v_{\rm sh} = +0.5$ V for $C_{\rm adj} = 22$ pF in Fig. 8(c), and $v_{\rm sh} = +1.3$ V for $C_{\rm adj} = 33$ pF in Fig. 8(d). From the simulation results of the new method, the range of $v_{\rm sh}$ was from -0.9 to $+1.3$ V, and the values were improved sharply from the value of -2.3 V for the simulation result without $C_{\rm adj}$.

TABLE II
SPECIFICATIONS OF THE AIR-CONDITIONING MOTOR

Components	Item (Unit)	Value
Motor	Input voltage (V_{dc})	200-391
	Maximum output power (W)	60
	Rated rotation speed (min^{-1})	1,000
	Rated torque (N-m)	0.3
	No. of poles	8
	No. of slots	12
	Rotor diameter (mm)	50.3
	Magnet length (mm)	24
	Stator outer diameter (mm)	87
	Stator inner diameter (mm)	50.9
	Stack length (mm)	13
Inverter	Switching frequency (kHz)	20
	modulation method	two-phase
Bearing (Type 608)	Base grease	Urea-based
	Kinematic viscosity [m^2/s](at 40℃)	53
	Outer diameter	22
	Inner diameter	8

In Fig. 8(b), the shaft voltage $v_{\rm sh}$ became about 0 V (-0.2 V) for $C_{\rm adj} = 15$ pF. Furthermore, from these results, it is clear that the bearing lubricant does not break down at 1000 $\rm min^{-1}$ because the breakdown voltage of 1000 $\rm min^{-1}$ is about 5 V from the results found in our previous papers [13].

C. Shaft Voltage Measurement

Fig. 9 shows the measurement results after inserting a 9–33-pF capacitor, where the dc link voltage was DC280 V, $v_{\rm com}$ was DC190 V, the motor speed was 1000 $\rm min^{-1}$, and two-phase PWM was used to drive the motor. Fig. 9(a) is the waveform for $C_{\rm adj} = 9$ pF and $v_{\rm sh} = -1.0$ V. Similarly, $v_{\rm sh} = -0.4$ V for $C_{\rm adj} = 15$ pF in Fig. 9(b), $v_{\rm sh}$ was at about 0 V for $C_{\rm adj} = 22$ pF in Fig. 9(c), and $v_{\rm sh} = +1.0$ V for $C_{\rm adj} = 33$ pF in Fig. 9(d).

From the measurement results of the new method, the range of $v_{\rm sh}$ was from -1.0 to $+1.0$ V, and the values were sharply improved from the value of -2.5 V for the measurement result without $C_{\rm adj}$, similar to the case of the simulation results.

Fig. 10 shows the comparison of $v_{\rm sh}$ between the simulation results and the measurement results. The simulation and measurement results agree well. From the figure, the validity of the equivalent circuit and the effects of $C_{\rm adj}$ can be verified.

From Figs. 8–10, one can find that further reduction of the shaft voltage is possible by using this new method. Therefore, broad adjustment can be made by addition of a commercial capacitor. That is, the shaft voltage can be reduced further than the original system without a capacitor in Fig. 2.

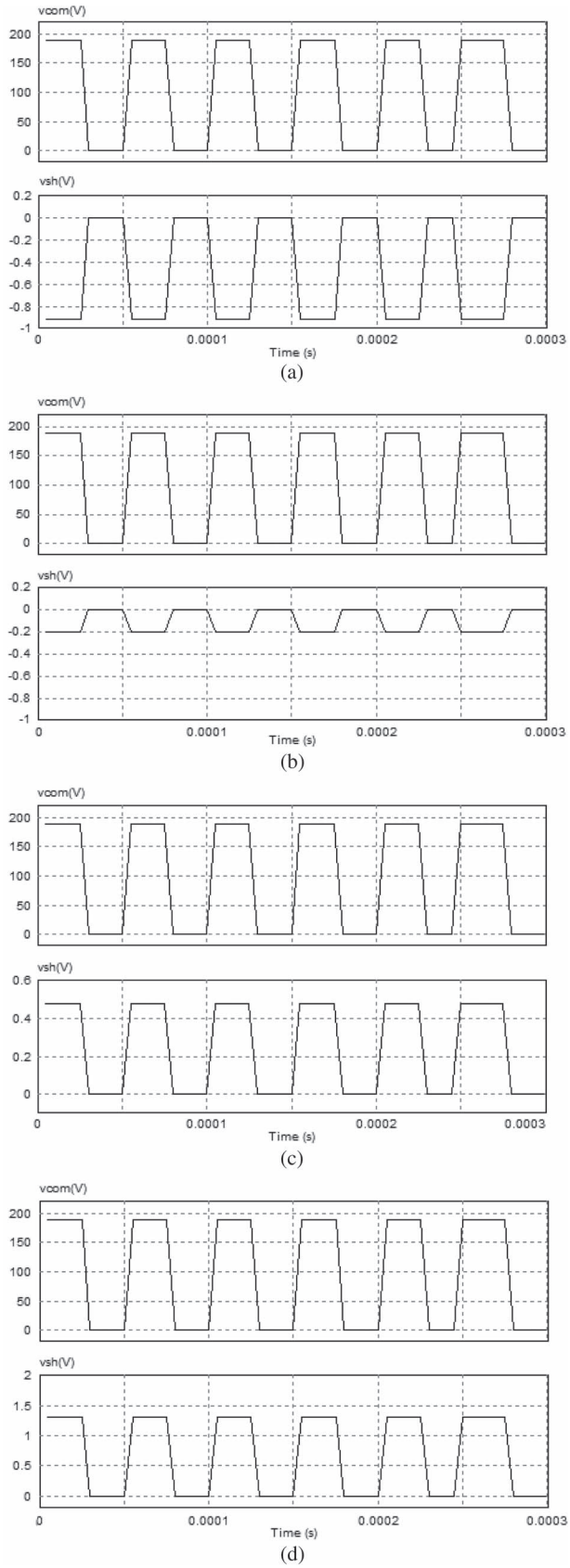

Fig. 8. Simulated waveforms of shaft voltage $v_{\rm sh}$. (a) $C_{\rm adj} = 9$ pF. (b) $C_{\rm adj} = 15$ pF. (c) $C_{\rm adj} = 22$ pF. (d) $C_{\rm adj} = 33$ pF.

IV. CONCLUSION

The new method of adding an adjusting capacitor $C_{\rm adj}$ between the bracket and the N line of a motor with an insulated rotor has been proposed to reduce the shaft voltage in the molded ungrounded BLDC motor. Also, its effectiveness for suppressing the shaft voltage was verified by simulation using a

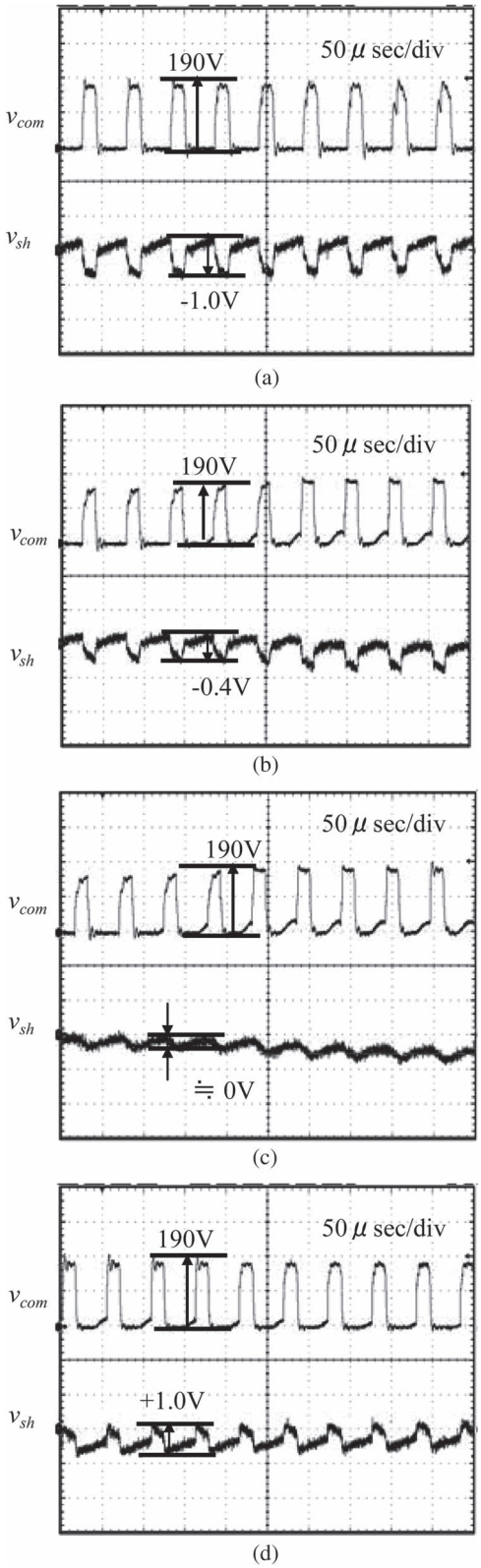

Fig. 9. Measured waveforms of shaft voltage $v_{\rm sh}$. (a) $C_{\rm adj} = 9$ pF. (b) $C_{\rm adj} = 15$ pF. (c) $C_{\rm adj} = 22$ pF. (d) $C_{\rm adj} = 33$ pF.

bridge-type common-mode simplified equivalent circuit. From the simulation results, the newly proposed method can reduce the shaft voltage to 1/25 by using an adjusting capacitor $C_{\rm adj}$. Additionally, the effects and validity were checked by the experimental results.

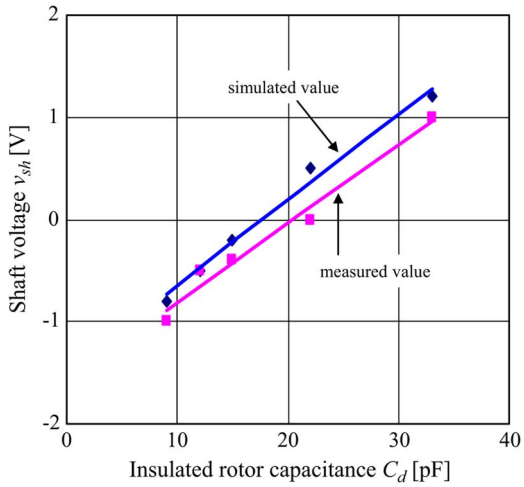

Fig. 10. Simulated and measured data of the shaft voltage.

We have clarified that it was possible to set the shaft voltage to 0 V through calculation by adding a capacitor when the equivalent circuit could be drawn.

REFERENCES

[1] S. Chen, T. A. Lipo, and D. Fitzgerald, "Modeling of motor bearing currents in PWM inverter drives," *IEEE Trans. Ind. Appl.*, vol. 32, no. 6, pp. 1365–1370, Nov./Dec. 1996.

[2] D. F. Busse, M. E. Erdman, R. J. Kerkman, D. W. Schlegel, and G. L. Skibinski, "An evaluation of the electrostatic shielded induction motor, a solution for rotor shaft voltage buildup and bearing current," *IEEE Trans. Ind. Appl.*, vol. 33, no. 6, pp. 1563–1570, Nov./Dec. 1997.

[3] S. Ogasawara, H. Ayano, and H. Akagi, "Active cancellation of the common-mode voltage produced by a voltage-source PWM inverter," *Inst. Elect. Eng. Jpn. Trans. Ind. Appl.*, vol. 117-D, no. 5, pp. 565–571, 1997.

[4] K. Yamada, H. Kirino, M. M. Swamy, and T. Kume, "Common-mode current attenuation techniques for use with PWM drives," in *Proc. Inst. Elect. Eng. Jpn. Ind. Appl. Soc. Conf.*, 1999, vol. III, pp. 75–78.

[5] K. Iimori, K. Shinohara, K. Yamamoto, and A. Morigami, "Approaches to suppressing shaft voltage in brushless dc motor driven by PWM inverter," *Inst. Elect. Eng. Trans. Ind. Appl.*, vol. 127-D, no. 4, pp. 406–411, 2007.

[6] T. Maetani, S. Morimoto, K. Iimori, Y. Isomura, and A. Watanabe, "Approaches to suppressing shaft voltage in brushless dc motor driven by PWM inverter," in *Proc. ICEMS*, Beijing, China, Aug. 20–23, 2011, pp. 1–6, PS-PMM-53.

[7] K. Tagami *et al.*, "Analysis of shaft voltage and bearing current in an inverter-fed nongrounded motor," *Inst. Elect. Eng. Jpn. Trans. Ind. Appl.*, vol. 127-D, no. 3, pp. 286–292, 2007.

[8] A. Muetze and A. Binder, "Calculation of motor capacitances for prediction of the voltage across the bearings in machines of inverter-based drive systems," *IEEE Trans. Ind. Appl.*, vol. 43, no. 3, pp. 665–672, May/Jun. 2011.

[9] R. Naik, T. A. Nondahl, M. J. Melfi, and R. Schiferl, "Circuit model for shaft voltage prediction in induction motors fed by PWM-based ac drives," *IEEE Trans. Ind. Appl.*, vol. 39, no. 5, pp. 1294–1299, Sep./Oct. 2003.

[10] O. Magdum, Y. Gemeinder, and A. Binder, "Investigation of influence of bearing load and bearing temperature on EDM bearing currents," in *Proc. ECCE*, Atlanta, GA, USA, 2010, pp. 2733–2738.

[11] A. Muetze and A. Binder, "Calculation of circulating bearing currents in machines of inverter-based drive systems," *IEEE Ind. Electron.*, vol. 54, no. 2, pp. 932–938, Apr. 2007.

[12] A. Muetze, J. Tamminen, and J. Ahola, "Influence of motor operating parameters on discharge bearing current activity," *IEEE Trans. Ind. Appl.*, vol. 47, no. 4, pp. 1767–1777, Jul./Aug. 2007.

[13] T. Maetani, S. Morimoto, K. Yamamoto, Y. Isomura, and A. Watanabe, "Influence of motor rotating speed on shaft voltage of brushless dc motor with insulated rotor driven by PWM inverters," in *Proc. SPEEDAM*, Sorrento, Italy, Jun. 20–22, 2011, pp. 730–735.

Yoshinori Isomura was born in Hyogo, Japan, in 1969. He received the B.E. degree in control engineering from Kyushu Institute of Technology, Fukuoka, Japan, in 1992.

He became an Engineer with Matsushita Electric Industrial Co., Ltd., Kadoma, Japan. Currently, his main research and development activities are motor control technologies at Panasonic Corporation, Daito, Japan.

Kichiro Yamamoto (M'97) was born in Japan in 1965. He received the B.E. and M.E. degrees from Kagoshima University, Kagoshima, Japan, in 1987 and 1989, respectively, and the Ph.D. degree from Kyushu University, Fukuoka, Japan, in 1996.

He was a Research Associate with Kagoshima National College of Technology, Kagoshima, from 1989 to 1993. Since then, he has been with the Department of Electrical and Electronics Engineering, Kagoshima University, where he is currently an Associate Professor. His research interests are ac motor drives and power converter circuits.

Dr. Yamamoto is a member of the Institute of Electrical Engineers of Japan.

Shigeo Morimoto (M'93) was born in Japan in 1959. He received the B.E., M.E., and Ph.D. degrees from Osaka Prefecture University, Sakai, Japan, in 1982, 1984, and 1990, respectively.

He joined Mitsubishi Electric Corporation, Tokyo, Japan, in 1984. Since 1988, he has been with the Graduate School of Engineering, Osaka Prefecture University, where he is currently a Professor. His main areas of research interest are permanent-magnet synchronous machines, reluctance machines, and their control systems.

Dr. Morimoto is a member of the Institute of Electrical Engineers of Japan, the Society of Instrument and Control Engineers of Japan, the Institute of Systems, Control and Information Engineers, and the Japan Institute of Power Electronics.

Tatsuo Maetani was born in Kagawa, Japan, in 1962. He received the B.E. and Ph.D. degrees from Osaka Prefecture University, Sakai, Japan, in 1984.

In 1984, he became an Engineer with Matsushita Electric Industrial Co., Ltd. Currently, his main research and development activities are motor control technologies at Panasonic Corporation, Daito, Japan.

Akihiko Watanabe was born in Fukui, Japan, in 1967. He received the B.E. degree in polymer engineering from Fukui University, Fukui, in 1989.

In 1989, he became an Engineer with Takefu Matsushita Electric Co., Ltd. Currently, his main research and development activities are motor component technologies at Panasonic Corporation, Daito, Japan.

Keisaku Nakano was born in Osaka, Japan, in 1979. He received the M.E. degree from Osaka University, Toyonaka, Japan, in 2003.

Since 2008, he has been an Engineer with Panasonic Corporation, Daito, Japan, where his research and development activities are tribology and high-performance materials for motors.